Thiol-Functionalized Gold Nanodots: Two-Photon Absorption Property and Imaging In Vitro

ARTICLE *in* THE JOURNAL OF PHYSICAL CHEMISTRY C · DECEMBER 2009

Impact Factor: 4.77 · DOI: 10.1021/jp9080492

Thiol-Functionalized Gold Nanodots: Two-Photon Absorption Property and Imaging In Vitro

Chien-Liang Liu,[†] Mei-Lin Ho,*[,‡] Yu-Chun Chen,[†] Cheng-Chih Hsieh,[†] Yi-Chih Lin,[†] Yu-Hsiu Wang,[†] Meng-Ju Yang,[†] Hsin-Sheng Duan,[†] Bo-So Chen,[†] Jyh-Fu Lee,[§] Jong-Kai Hsiao,[||] and Pi-Tai Chou*[,†]

Department of Chemistry, National Taiwan University, Taipei, Taiwan, Department of Chemistry, Soochow University, Taipei, Taiwan, National Synchrotron Radiation Research Center, Hsinchu 300, Taiwan, and Department of Medical Imaging, National Taiwan University Hospital and College of Medicine, Taipei, Taiwan

Received: August 20, 2009; Revised Manuscript Received: November 6, 2009

We report here the study of two-photon induced luminescence of 11-mercaptoundecanoic acid functionalized quantum-sized Au nanodots (11MUA-Au nanodots). The X-ray absorption near-edge structure (XANES) measurement at the gold L_{III} edge indicates that the oxidation state of the surface of 11MUA-Au nanodots is best described as Au^{+}. The two-photon absorption (TPA) property of 11MUA-Au nanodots was then investigated via an open aperture Z-scan method. Together with a precise extinction coefficient (i.e., one-photon absorption) extracted from inductively coupled plasma mass spectrometry, the TPA cross section, σ, was deduced to be 8761 ± 175 GM (800 nm) for 11MUA-Au nanodots (diameter 1.33 ± 0.12) in water. Upon dextran encapsulation, 11MUA-Au nanodots was proved to be highly water-soluble, stable, and low in toxicity, which demonstrated its power in two-photon imaging toward human mesenchymal stem cells (hMSCs) in vitro.

1. Introduction

During the past few years, much effort has been dedicated to the study of Au clusters due to their unique photophysical and photochemical properties.[1−4] Au clusters carry quantum-mechanical properties when their sizes are comparable to or smaller than the Fermi wavelength (∼1 nm) of conductive electrons. The resulting electronic energy states exhibit molecule-like transitions because densities of these states are too low to be qualified as bulk Au clusters.[5] This has allowed great potential to develop Au clusters as a new luminescence label.

Most research regarding emissive Au clusters has been focusing on the one-photon excitation properties. Some representative applications in, e.g., imaging can be referred to those works by Whetten and co-workers,[6] Huang et al.,[5a] and other groups.[7] Nonetheless, in several prospects, one-photon excitation cannot offer parallel performance compared to that of two photons. For example, the employment of two near-infrared photons for excitation offers several advantages over one-photon fluorescence in areas of three-dimensional optical data storage,[8] two-photon optical power limiting,[9] microfabrication,[10] and biological as well as medical applications. In particular, for in vitro imaging and photodynamic therapy,[11] two near-infrared photon excitation promotes penetration depth (>500 μm),[12,13a] fixed target excitation, and spatial resolution, and mitigates tissue autofluorescence, photodamage, and photobleaching. The two-photon absorption (TPA) cross sections of these Au or Ag clusters have been studied by two-photon-excited fluorescence or fluorescence upconversion method.[14] Although Au clusters with poor solubility and insufficient fluorescence quantum yield (10^{-7}−10^{-8}) made the two-photon cross section measurement challenging, these early approaches showed that Au clusters exhibited large two-photon cross sections. This unique property of efficient two photon absorbers is thus believed to provide an extensive application in biolabels.

Although there are considerable preceding researches in multiphoton imaging using the nonlinear properties of Au materials,[13,15] most involve colloidal gold[13i,15a,b] and anisotropic particles.[13b,e,f] Gold nanorods have received predominate attention because of their longitudinal plasmon modes resonating at the near-infrared region.[13d] Combined with the advantage of reduced plasmon damping effect, the suitability of gold nanorods being a two-photon luminescence agent has previously been demonstrated both in vitro and in vivo.[13d] Recent advancement includes folate-conjugated plasmon-resonant gold nanorods capable of being monitored in real time by two-photon luminescence microscopy while acting as a photothermal agents in biological systems.[13a] Other diverse utilizations of gold nanomaterials in imaging include employing them as bright contrast agents for two-photon imaging of cancer cells deep in a tissue phantom,[15c] or as a nanolens to amplify the weak intrinsic multiphoton processes occurring in proximity.[13c]

Despite the intense research in larger size (>10 nm) gold nanomaterials,[13,15] multiphoton excitation, such as TPA and/or two-photon excited emission utilizing Au clusters is scant; applications of two-photon cell imaging using emissive Au clusters, in particular, are pending exploration.[14a] Herein, upon surface modification by 11-mercaptoundecanoic acid (11MUA), we report the preparation of highly fluorescent and water-soluble Au nanodots (11MUA-Au nanodots). The one-photon absorption cross section, i.e., the extinction coefficient, of 11MUA-Au nanodots was then carefully determined by transmission electron microscopy (TEM) in combination with inductively coupled

* To whom correspondence should be addressed. Mailing address: Department of Chemistry, National Taiwan University, Taipei 106, Taiwan. Fax: +886-2-23695208. Tel: +886-2-33663894. E-mail: chop@ntu.edu.tw (P.-T.Chou); meilin_ho@scu.edu.tw (M.-L.Ho).
† National Taiwan University.
‡ Soochow University.
§ National Synchrotron Radiation Research Center.
|| National Taiwan University Hospital and College of Medicine.

10.1021/jp9080492
Published on Web 11/19/2009

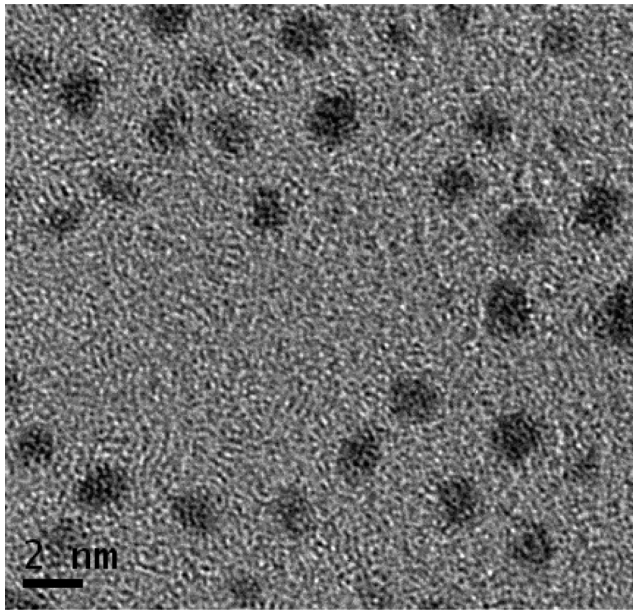

Figure 1. TEM images of 11MUA-Au nanodots; 100 particles were randomly selected for the size distribution measurement, which was determined to be 1.33 ± 0.12 nm in diameter.

plasma mass spectrometry (ICP-MS). Subsequently, the TPA property was investigated via both two-photon induced emission and Z-scan methods. To analyze the surface electronic structure of 11MUA-Au nanodots, we also performed X-ray absorption near-edge structure (XANES) measurement at the Au L_{III} edge. The results gathered have gained more insight into the associated photophysical phenomena as well as the surface electronic configuration. From the application viewpoint, we then successfully demonstrated two-photon induced fluorescence imaging in vitro with human mesenchymal stem cells (hMSCs) using these stable and biocompatible Au nanodots.

2. Experimental Section

Synthesis of 11MUA Functionalized, Quantum-Size Au Nanodots (11MUA-Au Nanodots). The synthesis of aqueous 11MUA-Au nanodots took reference from Huang et al.[5a] The Au nanodots was prepared through reduction of Au with tetrakis(hydroxymethyl)phosphonium chloride (THPC, 10 μL) from hydrogen tetrachloroaurate (III) trihydrate ($HAuCl_4 \cdot 3H_2O$, 50 mM, 1 mL) in buffer sodium tetraborate at pH 9.2. By reacting with 11MUA (100 mM, 1 mL) for 24 h in the dark at room temperature, 11MUA-Au nanodots was generated and then purified by centrifugation (4,300 *g*, 5 min) with an Amicon centrifuge filter (10 kDa MWCO, Millipore). The size of the 11MUA-Au nanodots was determined by TEM (Hitachi H-7100). TEM analysis of the solution discovered the presence of small nanodots with homogeneous size distribution (see Figure 1). Further information is given by the histogram analysis (see Supporting Information, Figure S1), the result of which indicated that the size distribution of 11MUA-Au nanodots has a mean diameter of 1.33 nm. Note that the histograms regarding the particle size distribution are constructed on the basis of four TEM photographs, and a total of 100 particles are used in this histogram.

The Extinction Coefficient of Au Nanodots. The concentration of the samples used in two-photon excitation fluorescence (TPEF) or Z-scan experiments cannot be deduced without precise measurement of the extinction coefficient of 11MUA-Au nanodots. This task involves both ICP-MS and TEM studies. The analysis of 11MUA-Au nanodot concentration was conducted using ICP-MS (Agilent 7500ce) at the Center of Instrumentation Center, National Tsing Hua University. Combining the result from ICP-MS and the method suggested by Liu et al.,[16] the extinction coefficient of the 11MUA-Au nanodots was calculated (see also Supporting Information). The sample was prepared by microwave digestion with a CEM MARS 5 microwave digestion system (CEM Co., Ltd., USA), including a microwave oven, PTFE/TFE high pressure vessels, and a fixed tray. Deionized water (Milli-Q ultrapure water system) was used. A Babington nebulizer was fitted to a PDF Quartz Scott-type spray chamber. The concentration of 11MUA-Au nanodots was determined by averaging three measurements. The instrumental operating conditions for optimal sensitivity and low background noise are presented in Table S1 (see Supporting Information).

Spectral Measurement. Steady-state absorption and emission spectra of 11MUA-Au nanodots were recorded with a Hitachi (U-3310) spectrophotometer and an Edinburgh (FS920) fluorimeter, respectively. Both wavelength-dependent excitation and emission response of the fluorimeter were calibrated. To measure the emission quantum yield, Coumarin 480 in methanol with quantum yield of ~0.87 served as the standard.[17a] Lifetime study was performed with an Edinburgh FL900 photon-counting system with a hydrogen-filled or nitrogen lamp as the excitation source. Data were analyzed by using the nonlinear least-squares procedure in combination with an iterative convolution method. The emission decay was analyzed by the sum of exponential functions, which allows partial removal of the instrument time broadening and provides a temporal resolution of approximately 300 ps.

XANES Measurement. X-ray absorption experiment was carried out at the National Synchrotron Radiation Research Center (NSRRC), Hsinchu, Taiwan. All spectra of the Au L_{III} edge were recorded at room temperature at the superconducting wavelength shifter beamline of 01C1 with a double Si(111)-crystal monochromator. The energy resolution $\Delta E/E$ was about 1.6×10^{-4}. High harmonics were removed using Pt-coated mirrors. XANES spectra of 11MUA-Au nanodots and reference Au salts in solution were recorded in fluorescence mode, and the reference Au(0) foil was measured in transmission mode. The XANES spectra were processed via a pre-edge background subtraction followed by a normalization procedure described in the literature.[17b] The spectra of the reference compounds, $HAuCl_4 \cdot 3H_2O$ and (dimethylsulfide)-gold(I) chloride, were recorded in transmission mode. $HAuCl_4 \cdot 3H_2O$ was purchased from Sigma-Aldrich. The synthesis of (dimethylsulfide)-gold(I) chloride took reference from Brandys et al.[17c] Energy calibration of all spectra was based on Au(0) foil at 11919 eV.

Measurement of a Two-Photon Cross Section by TPEF Technique. The setup for TPEF spectra and TPEF cross section measurement has been described in our previous report.[17a,18] In brief, a femtosecond mode-locked Ti:sapphire laser (Spectra Physics) generated ~100 fs pulses at a repetition rate of 82 MHz with an average power of 300−400 mW. The laser beam was focused on a sample cell (1 cm) by a lens with the focal length of 6 cm. To minimize the effects of reabsorption, the excitation beam was focused as close as possible to the wall of the quartz cell, which faced the slit of the imaging spectrograph. Two-photon induced fluorescence was detected at a direction perpendicular to the pump beam. The fluorescence was collected at a right angle with respect to the excitation beam, directly focused to a monochromator (Acton, SP2300i) and then detected by a highly sensitive intensified charge coupled detector (ICCD,

Princeton Instrument, PI-MAX camera). TPA and TPEF cross sections (δ and δ_e, respectively) are basic parameters to evaluate TPA and TPEF properties of a material. From TPEF intensity data, δ_e and δ can be evaluated by using eqs 1 and 2,[19] where r is the reference compound, n is the refractive index of solvents applied, F is the integrated fluorescence intensity, and C is the concentration of the molecules in solution.

$$\delta_e = \delta_{e,r}\frac{Fn_rC_r}{F_rnC} \quad (1)$$

$$\delta\Phi = \delta_e \quad (2)$$

The TPEF cross section δ_e is linearly dependent on the TPA cross section (δ) and the TPEF quantum yield Φ'. In most reports, the single photon excitation fluorescence quantum yield Φ was adopted instead of Φ' because Φ' is difficult to measure. The TPEF cross section was referencing by the TPEF cross section of Coumarin 480 to be 146.3 ± 3 GM (1 GM = 10^{-50} cm^4 s/photon).[20]

Measurement of the TPA Cross Section by an Open Aperture Z-Scan Method. The TPA cross section of 11MUA-Au nanodots at 800 nm was measured by an open aperture Z-scan experiments.[21a,b] A mode-locked Ti:sapphire laser (Tsunami, Spectra Physics) produced single Gaussian pulse (800 nm) which was coupled to a regenerative amplifier that generated approximately 180 fs and 1 mJ pulse (760−840 nm, 1 kHz, Spitfire, Spectra Physics). To circumvent the build up of excited-state populations, we further reduced the output of our amplifier to 10 Hz. Pulse energy, after appropriate attenuation, was reduced to 0.5−0.7 μJ. After passing through an f = 30 cm lens, the laser beam was focused and passed through a 2.00 mm cell (2.3×10^{-5}∼1.7×10^{-4} M), and the beam radius at the focal position was 3.40×10^{-3} cm. When the sample cell changed its position along the beam direction (z-axis), the transmitted laser beam from the sample cell was detected by a photodiode (PD-10, Ophir). Accordingly, in theory, the TPA-induced decrease of transmittance, $T(z)$, can be expressed as eqs 3 and 4, and the TPA coefficient (β) can be obtained from experimental data by fitting Z-scan curves to eqs 3 and 4.

$$T(z) = \sum_{n=0}^{\infty}\frac{(-q)^n}{(n+1)^{3/2}} \quad (3)$$

$$q = \frac{\beta I_0 L}{1+\frac{z^2}{z_0^2}} \quad (4)$$

where n is an integer number from 0 to ∞ and has been truncated at n = 1000, L is the sample length, I_0 is the input intensity, and z_0 is the diffraction length of the incident beam (Rayleigh range).[21a,b] After obtaining the TPA coefficient (β), the TPA cross section (σ) can be deduced by using eq 5, where N_A is the Avogadro constant, d is the concentration, h is the Plank constant, and v is the frequency of the incident beam. The error of TPA measurement by the Z-scan method was in the range of <5% (five replicas).

$$\beta = \frac{\sigma N_A d \times 10^{-3}}{h\nu} \quad (5)$$

To counter the hidden aperture effect in Z-scan measurements, in which the excitation energy is lost due to self-defocusing, we have placed another focusing lens (f = 5 cm) 25 cm away from the focal point and 10 cm in front of the photodiode to collect the transmitted light. Before data acquisition, we have made certain that the transmitted beam, especially when the sample was moved to the focal point, completely fitted in the detecting region of the photodiode head.

Dextran-Coated 11MUA-Au Nanodots. The synthesis of dextran-coated 11MUA-Au nanodots took reference from Lee et al.[21c] To partially exchange the −COOH of 11MUA to −OH, 11MUA Au nanodots and 20 mM 1-ethyl-3-(3-dimethylaminopropyl)-carbodiimide (EDC) were reacted for 10 min. Then, 100 mM 2-(2-aminoethoxy)ethanol (AEE) in double distilled water was added and reacted for 2 h. Unreacted AEE was removed by centrifugal filtration (4500 g, 10 min) with a Amicon centrifuge filter (Millipore) having a 10 kDa molecular weight cut off. In order to introduce active epoxide groups, the hydroxyl-functionalized nanodots were reacted with 100 mM epichlorohydrin in a 1:1 mixture of diglyme and 0.4 M NaOH for 4 h. The nanodots was purified by centrifugal filtration at 4500 g for 10 min again and resuspended in water. Afterward, the gold nanodots were further reacted with dextran solution (50 mg/mL in 0.1 M NaOH) overnight and then repetitively centrifuged (4500 g, 10 min) and resuspended in water to remove unreacted dextran. The dextran-coated 11MUA-Au nanodots were collected for cell cytotoxicity test and uptake.

In Vitro Test. In the test of cytotoxicity of dextran-coated 11MUA-Au nanodots, human mesenchymal stem cell line (hMSCL) was adopted as a target for biomedical imaging. This cell line was cultured in 10 cm Petri dishes (BD) with Dulbecco's modified Eagle's medium (DMEM, Sigma) supplemented with 10% fetal bovine serum (Hyclone) and 1% penicillin/streptomycin (Sigma). All cultures were kept in moist atmosphere of 5% CO_2, 95% air at 37 °C. Cells were passaged through trypsinization, and nucleated cells were centrifuged at 100 g for harvesting. For cytotoxicity test, cells were seeded in a 24 well plate at 5×10^3 cell/well density in 500 μL culturing medium 24 h prior to particle feeding. Different amounts of 11MUA-Au were placed in each well to reach final concentrations of 0, 6.25, 12.5, 25, 50, and 100 μg/mL. After 24 h of incubation, each well was washed with phosphate buffered saline (PBS: 137 mM NaCl, 2.68 mM KCl, 10 mM Na_2HPO_4, 1.76 mM KH_2PO_4, pH 7.4) twice, and replenished with 500 μL culturing medium with 10% of 3-(4,5-dimethylthiazol-2-yl)-2,5-diphenyltetrazolium bromide (MTT) agent. After 1 h of incubation and medium removal, the newly formed purple MTT-formazan was dissolved in 200 μL dimethyl sulfoxide (Sigma), and the absorbance was measured at 570 nm by a spectrophotometer (Tecan Infinite F200).

For two-photon and confocal microscopic study, hMSCs were seeded on 0.17 mm coverslips placed in a 6 well plate at 5×10^4 cell/well density in 2 mL of culturing medium 24 h prior to particles feeding. After 24 h incubation with 25 μg/mL of dextran-coated 11MUA-Au nanodots, cells were washed three times with PBS and then fixed in a 3.7% paraformaldehyde solution in PBS at room temperature for 5 min. The cells were then washed twice with PBS and incubated with 0.5% Triton X-100 (Sigma-Aldrich) plus 1% bovine serum albumin (BSA; Sigma-Aldrich) in PBS at room temperature for 5 min. 4′,6-Diamidino-2-phenylindole (DAPI; Molecular Probes) and rhodamine phalloidin (Invitrogen) were used in this optical microscopic study for nucleus and cytoskeleton labeling, respectively. DAPI staining (5 μg/mL) in PBS for 10 min at room temperature came after cell samples were completely washed with PBS two or more times. Afterward, 7.5 μL of methanolic stock solution of rhodamine phalloidin was diluted into 1 mL of PBS and used for actin staining for 20 to 30 min. Cell samples were washed twice with PBS and then examined

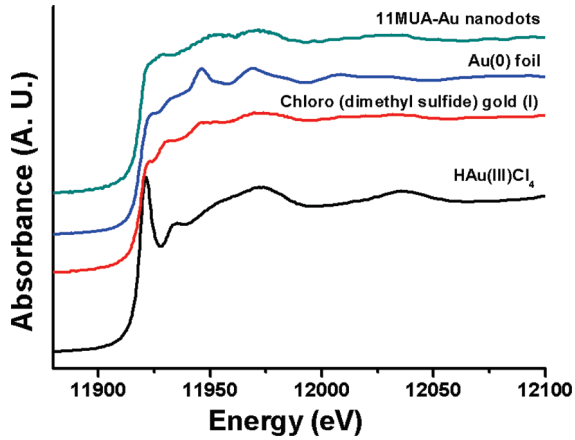

Figure 2. Normalized XANES spectra for 11MUA-Au nanodots together with Au(0) foil, (dimethylsulfide)-gold(I) chloride, and $HAu(III)Cl_4$ reference materials.

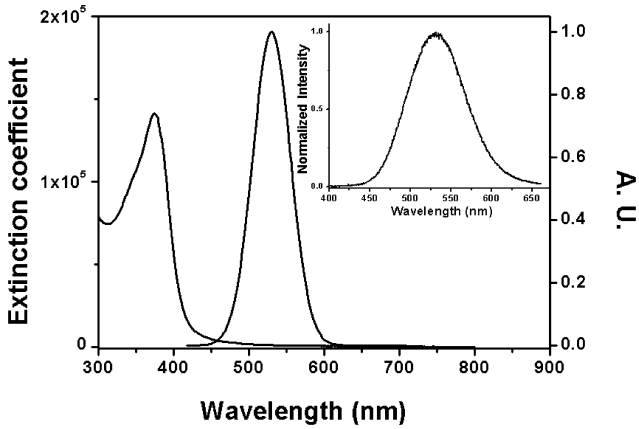

Figure 3. UV/vis absorption and emission spectra of 11MUA-Au nanodots in water. $\lambda_{ex} = 360$ nm. Inset: two-photon induced fluorescence spectra of 11MUA-Au nanodots under 800 nm excitation.

by a Zeiss LSM710 Inverted Confocal Spectral Microscope equipped with either a X40 (C-Apo, NA 1.2, water immersion) or a X63 (Plan-Apo, NA 1.4, oil immersion) objective. A tunable femtosecond (~100 fs) pulse laser (Mai Tai DeepSee, Spectra-Physics) and a 543 nm He−Ne laser were employed as the excitation sources.

3. Results and Discussion

3.1. XANES Analyses. To provide evidence for the surface electronic structure of the as prepared 11MUA functionalized Au nanodots in water, XANES measurement was performed at the Au L_{III} edge. Figure 2 shows the XANES spectra of 11MUA-Au nanodots in water, together with Au(0) foil, chloro(dimethyl sulfide) gold(I) and $HAu(III)Cl_4$ reference materials. The first resonance at the edge is often known as the white line, arising from $2p_{3/2} \rightarrow 5d$ dipole transition, the intensity of which is related to the density of unoccupied densities of *d* states (*d* hole counts) above the Fermi level. As for the XANES spectrum of 11MUA-Au nanodots, the presence of a weak but discernible white line is in line with an observation by Zhang et al.[17b] They infer that the *d*-charge redistribution of thiol-capped Au results in lattice relaxation, which is a balance of the nanosize effect (contraction) and, as importantly, interfacial charge transfer through the Au−S bonding. A similar result has also been reported by Murray and co-workers, where the surface of Au monolayer-protected clusters (MPCs) bears a partial positive charge.[22] Recently, similar assignment has also been made by Huang et al.[5f] by using X-ray photoelectron spectroscopy.

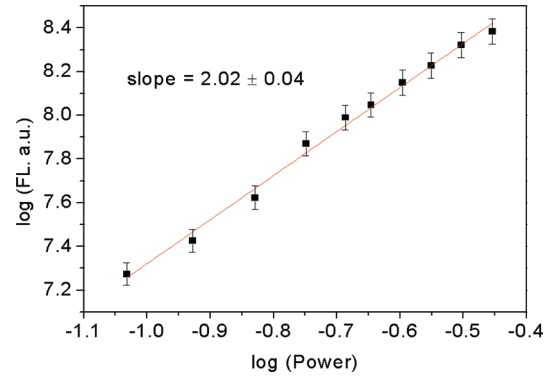

Figure 4. Power dependence of fluorescence for 11MUA-Au nanodots in water obtained by two-photon excitation at 800 nm.

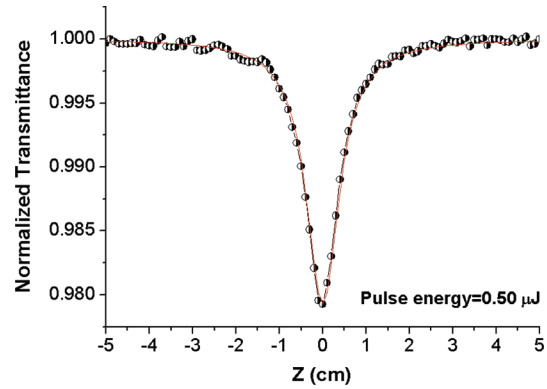

Figure 5. Z-scan experimental data (in water, pH ~ 7) of 11MUA-Au nanodots (1.7×10^{-4} M) (circles), in a 2-mm thickness cell. Solid lines are the result of a fit to the data points.

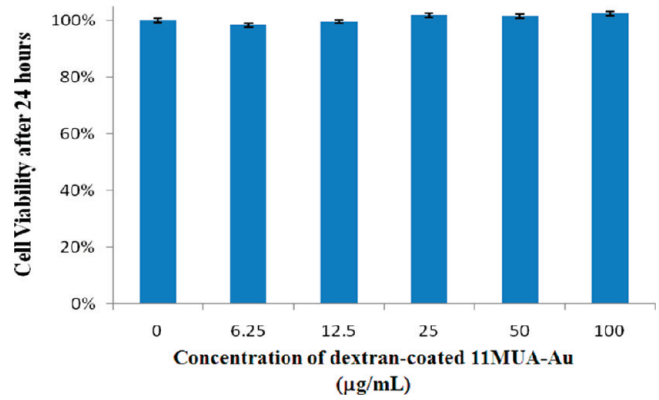

Figure 6. The viability of hMSCL after treating with different concentrations of dextran-coated 11MUA-Au nanodots (0, 6.25, 12.5, 25, 50, 100 μg/mL) for 24 h. The viability was obtained by MTT test. Error bar represents standard error of four trials.

3.2. Photophysical Properties. Steady state absorption and emission spectra of 11MUA-Au nanodots were acquired to initiate the photophysical property investigation (Figure 3). As accuracy of one photon extinction coefficient was believed to be necessary for the simplicity and precision of sample preparations for the later two-photon experiments, the absorption extinction coefficient of 11MUA-Au nanodots was carefully conducted. The absorption spectrum of 11MUA-Au nanodots exhibits a broadband spanning from ultraviolet to visible region and maximizes at 375 nm. Calculated by Beer's law, in which the concentration of 11MUA-Au nanodots was deduced from ICP-MS in combination with TEM measurements,[16] the extinction coefficient was found to be 1.30×10^5 at 375 nm (see Experimental Section and Supporting Information). The spectral

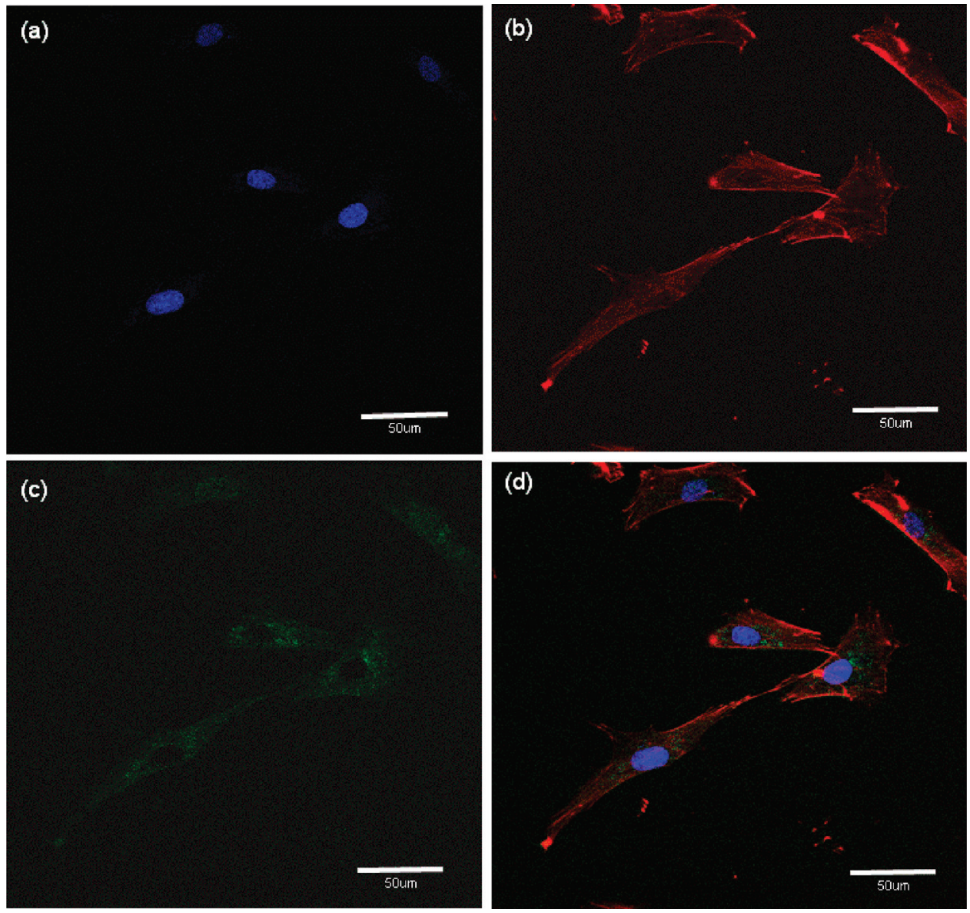

Figure 7. Microscopic observation of the dextran-coated 11MUA-Au nanodots internalization. hMSCs were treated with dextran-coated 11MUA-Au nanodots for 24 h and then processed for two-photon and confocal microscopic examination. (a) Cell nucleus was stained with DAPI (blue color). (b) Actin fiber was stained with rhodamine phalloidin to confirm the cell boundary (red color). (c) Dextran-coated 11MUA-Au nanodots exhibit a two-photon emission (green luminescence) for in vitro bioapplication. (d) Fluorescence image overlay of the three images demonstrating the internalization of 11MUA-Au nanodots residing near the nucleus.

profile of Au nanodots was in close resemblance to those of small Au MPCs[23a−f,i] and Au nanodots.[5f,23g] On the basis of previous reports,[5f,6b] the absorption bands can be ascribed to the interband transitions from the Au $5d^{10}$ levels to the unoccupied Au $6(sp)^1$ band, although metal−ligand charge transfer may have also contributed to the fine details of the spectra. Additionally, no surface plasmon resonance band around 520 nm was observed, suggesting that the sizes of the Au nanodots were smaller than 2 nm.[24] As for the fluorescent spectrum of 11MUA-Au nanodots in water, upon excitation at, e.g., 360 nm, Au nanodots exhibit a narrow and intense emission band with an emission peak at 530 nm. The emission quantum yield for 11MUA-Au nanodots was measured to be 3.1×10^{-2}. Note that these values are larger by ~5 orders of magnitude than that of Au_{25} (~10^{-7})[14a] and should be more suitable for two-photon imaging applications (vide infra). Both absorption and emission spectral features observed were in agreement with previous results.[5a] However, the origin of luminescence is intriguing but somewhat complicated.[5a,6b,3e] As mentioned in the previous section, our XANES analysis at the Au L_{III} edge suggested that the surface oxidation state of 11MUA-functionalized Au nanodots is best described as Au^+. Therefore, we lean toward adopting the Au^+ relevant mechanism, which may be associated with metal (Au^+)−ligand type of transition, as a possible source for emission. More recently, the origin of luminescence has been suspected from Au nanodots/polynuclear Au(I)−thiol (core/shell) complexes.[5g]

3.3. TPA Properties. To achieve the goal of employing the as-prepared 11MUA-Au nanodots in bioimaging, we have thoroughly investigated its TPA properties in neutral water. Two maneuvers were adopted to achieve the task, namely, the two-photon emission spectra and Z-scan measurements, both of which would be complementary so the resulting data could be mutually affirmed.

As displayed in inset of Figure 3, two-photon emission spectra obtained after excitation at 800 nm showed an emission color of green with a maximum at 530 nm. This result was consistent with one-photon excitation emission in respect to peak wavelength and spectral profile. The corresponding pump power dependence of the emission at 530 nm for 11MUA-Au nanodots, which was linearly dependent on the square of the incident laser power, firmly supported the occurrence of two-photon excitation (see Figure 4). Recently, Ramakrishna et al.[14a] reported Au_{25} with high TPA cross section, but its poor solubility in water and low total fluorescence impeded the applicability as biolabels. Furthermore, the Au clusters with insufficient fluorescence quantum yield (10^{-7}−10^{-8}) made the two-photon cross section measurement challenging. Conversely, 11MUA-Au nanodots reported here feature relatively high one-photon quantum yield, which allows them not only to serve as suitable two-photon absorbers, but also facilitate the precise two-photon cross section determination.

The TPA cross section, in one approach, was measured using TPEF technique, in which a femtosecond (~100 fs, 750−840 nm) Ti-sapphire laser was used for the measurement in order to eliminate any contribution from the single photon resonance excitation. Comparative TPA cross section measurement was

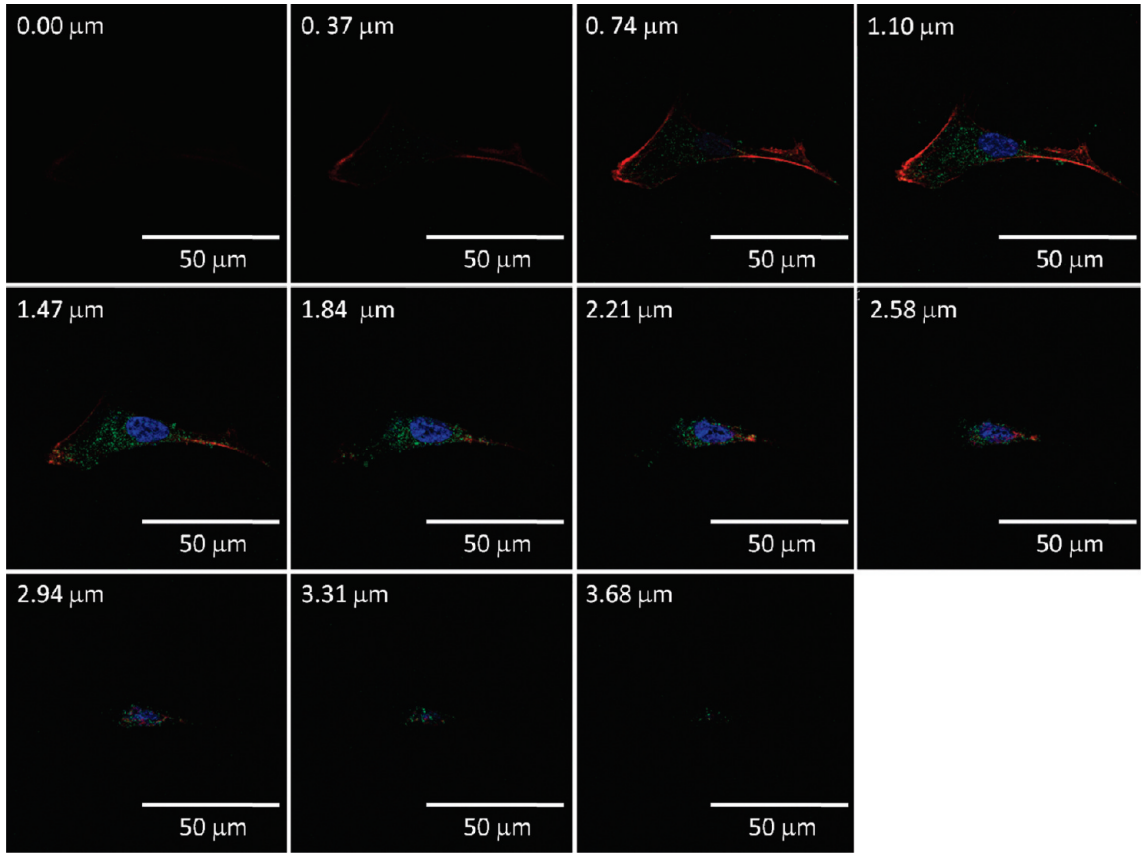

Figure 8. Confocal Z-stack sectioning of hMSC treated with 25 μg/mL dextran-coated 11MUA-Au nanodots 24 h. Cells were fixed with 4% paraformaldehyde, stained with DAPI for nucleus (blue), and rhodamine phalloidin for actin filament (red). A femtosecond pulse laser at 800 nm was used as the excitation source for the nanodots.

used to determine the TPA cross section by referencing Coumarin 480 in methanol.[20] As a result, the TPA cross section of 11MUA-Au nanodots in water solution was measured to be 3426 ± 70 GM (at 800 nm). Alternatively, open-aperture Z-scan method with 1 kHz femtosecond laser, which could reduce the excited-state reabsorption, was also performed to determine the TPA cross section based on changes of the transmittance along the Z-scan (see Figure 5 and experimental section for detail). The TPA cross section of Au nanodots deduced from Z-scan method was 8761 ± 175 GM (800 nm). To discuss this discrepancy, we first acknowledge that the Z-scan method can lead to some overestimation of TPA cross section. As for circumventing the build up of excited-state populations, in this study, we have reduced the output of our amplifier to 10 Hz. On the other hand, we view the difference of TPA cross section obtained from the TPEF method, which is approximately 55% of that obtained from Z-scan, resulting from the build up of excited-state populations and the subsequent reabsorption or ground state bleaching. The problem can be especially considerable when a current setup of 82 MHz repetition rate (excitation laser) is applied to a system with lifetime of >100 ns, such as 11MUA-Au nanodots.[21d] Nevertheless, the results of both methods indicate that a two-photon cross section of 11MUA-Au nanodots in water surpasses most water-soluble fluorophores and is comparable to that of quantum dots.[25] Since the free electrons of Au nanodots (or clusters), in theory, should exhibit great polarizability upon moving around the cluster, the result of a large TPA cross section might be expected.[14b] To provide a measure for practical use in two-photon imaging, we take the product of the TPA cross section (δ) and emission quantum yield (Φ), which is equivalent to the TPEF cross section (δ_e). Inserting the average δ value of those obtained from Z-scan and TPEF measurements (6094 GM) and 0.031 for Φ, a value of 189 GM is deduced when excited at 800 nm. With the advantages of water-soluble, large two-photon cross section, small size, and excellent one- and two-photon brightness, 11MUA-Au nanodots hold great promise as high sensitivity biolabels depicted as follows.

3.4. Two-Photon Emission Imaging In Vitro. High-level of biocompatibility is the key of success when applying nanodots in vitro. Bearing this aim in mind, we successfully coated 11MUA-Au nanodots with dextran while retaining its luminescence properties, as evidenced by the nearly identical emission yield of 0.03 after modification. The biocompatibility of dextran-coated Au nanodots was ensured in two ways: negligible cellular toxicity from cell proliferation test, and the preservation of two-photon signal after internalization into the cell as observed under a confocal microscopy. In this approach, hMSCL was selected as the testing candidate because of its increasing importance in biomedical field due to its multipotent differentiation ability. The results depicted in Figure 6 clearly indicate that the cells prescribed with final concentrations of 0, 6.25, 12.5, 25, 50, and 100 μg/mL dextran-coated 11MUA-Au nanodots remained almost 100% viable even after 24 h of incubation period, demonstrating the negligible cytotoxicity of the as-prepared nanodots. It is not surprising since dextran has long been recognized as biocompatible material and applied in various medial applications.[26] The innocuous dextran-coated 11MUA-Au nanodots is therefore considered to be adequate in cellular imaging. As for the two-photon imaging in vitro, fixed cell samples were imaged with a nonlinear confocal microscope with 800 nm pulse laser (pulse duration of ~100 fs) to avoid severe

interference from cell autofluorescence under, e.g., 488 nm excitation. Even though certain reports suggested that stem cells possess strong autofluorescence under high power pulse laser,[27] the large TPA cross section and sufficient quantum yield of 11MUA-Au nanodots surpassed this hamper. Figure 7 shows the merged (see Figure 7d) and individual channels of confocal images of the hMSCs treated with 25 μg/mL dextran-coated 11MUA-Au nanodots for 24 h; for contrast enhancement, cell nucleus was stained with DAPI (blue color, Figure 7a) and the actin fibers were stained with rhodamine phalloidin to confirm the cell boundary (red color, Figure 7b). Figure 7c shows that dextran-coated 11MUA-Au nanodots exhibit a green luminescence via two-photon excitation in vitro. Appropriate dye separation was carefully performed to avoid the potential interference of dextran-coated 11MUA-Au nanodots' signal from DAPI under 800 nm two-photon laser. Under microscopy, cells appeared intact, and their native morphology was highly retained. In addition, the Z-stack sectioning reveals that dextran-coated 11MUA-Au nanodots (green luminescence) were internalized into the cells and mainly resided in the cytoplasm nearby the nucleus (Figure 8). The result is in accordance with the endocytosis of nanoparticles reported previously.[28] The high biocompatibility demonstrated here validates the applicability of dextran-coated 11MUA-Au nanodots in two-photon imaging.

4. Conclusion

In summary, 11MUA attaching onto the surface of Au nanodots for the preparation of highly fluorescent and water-soluble metal nanodots was achieved. We present in our study of using UV−vis absorption spectroscopy and ICP-MS to precisely determine the extinction coefficient of 11MUA-Au nanodots, which is critical for accurate sample preparation for optical measurements. TPA cross section of Au nanodots was measured from both TPEF and Z-scan methods, for which two-photon cross sections in water surpass many known water-soluble fluorophores and are comparable to that of quantum dots. For practical application, labeling capability and biocompatibility of dextran-coated Au nanodots was successfully demonstrated in vitro using hMSCs with two-photon confocal microscopy. Although the structure of Au nanodots requires further studies, this new type of TPA absorber holds promise for applications in biological labeling.

Acknowledgment. This work was funded by the National Science Council of Taiwan, ROC (NSC97-3114-M-002-003).

Supporting Information Available: Histogram analysis of 11MUA-Au nanodots, operation conditions for the ICP-MS system, derivation of 11MUA-Au nanodot concentration, and extinction coefficient calculation of 11MUA-Au nanodots. This material is available free of charge via the Internet at http://pubs.acs.org.

References and Notes

(1) (a) Abad, J. M.; Sendroiu, I. E.; Gass, M.; Bleloch, A.; Mills, A. J.; Schiffrin, D. J. *J. Am. Chem. Soc.* **2007**, *129*, 12932. (b) Dass, A.; Stevenson, A.; Dubay, G. R.; Tracy, J. B.; Murray, R. W. *J. Am. Chem. Soc.* **2008**, *130*, 5940. (c) Link, S.; El-Sayed, M. A.; Schaaff, T. G.; Whetten, R. L. *Chem. Phys. Lett.* **2002**, *356*, 240. (d) Pyykkö, P. *Angew. Chem., Int. Ed.* **2004**, *43*, 4412.

(2) (a) Shichibu, Y.; Negishi, Y.; Watanabe, T.; Chaki, N. K.; Kawaguchi, H.; Tsukuda, T. *J. Phys. Chem. C* **2007**, *111*, 7845. (b) Sevillano, P.; Fuhr, O.; Hampe, O.; Lebedkin, S.; Matern, E.; Fenske, D.; Kappes, M. M. *Inorg. Chem.* **2007**, *46*, 7294. (c) Schulz-Dobrick, M.; Jansen, M. *Angew. Chem., Int. Ed.* **2008**, *47*, 2256. (d) Schmid, G. *Angew. Chem., Int. Ed.* **2008**, *47*, 3496. (e) Heaven, M. W.; Dass, A.; White, P. S.; Holt, K. M.; Murray, R. W. *J. Am. Chem. Soc.* **2008**, *130*, 3754. (f) Liu, Z.; Peng, L.; Yao, K. *Mater. Lett.* **2006**, *60*, 2362. (g) Spiekermann, A.; Hoffmann, S. D.; Kraus, F.; Fässler, T. F. *Angew. Chem., Int. Ed.* **2007**, *46*, 1638. (h) Woehrle, G. H.; Brown, L. O.; Hutchison, J. E. *J. Am. Chem. Soc.* **2005**, *127*, 2172.

(3) (a) Lechtken, A.; Schooss, D.; Stairs, J. R.; Blom, M. N.; Furche, F.; Morgner, N.; Kostko, O.; von Issendorff, B.; Kappes, M. M. *Angew. Chem., Int. Ed.* **2007**, *46*, 2944. (b) Yoon, B.; Koskinen, P.; Huber, B.; Kostko, O.; von Issendorff, B.; Häkkinen, H.; Moseler, M.; Landman, U. *ChemPhysChem* **2007**, *8*, 157. (c) Kim, J.; Lee, D. *J. Am. Chem. Soc.* **2007**, *129*, 7706. (d) Guliamov, O.; Frenkel, A. I.; Menard, L. D.; Nuzzo, R. G.; Kronik, L. *J. Am. Chem. Soc.* **2007**, *129*, 10978. (e) Eichelbaum, M.; Schmidt, B. E.; Ibrahim, H.; Rademann, K. *Nanotechnology* **2007**, *18*, 355702.

(4) (a) Jadzinsky, P. D.; Calero, G.; Ackerson, C. J.; Bushnell, D. A.; Kornberg, R. D. *Science* **2007**, *318*, 430. (b) Schulz-Dobrick, M.; Jansen, M. *Z. Anorg. Allg. Chem.* **2007**, *633*, 2326. (c) Ueno, K.; Juodkazis, S.; Mizeikis, V.; Sasaki, K.; Misawa, H. *Adv. Mater.* **2008**, *20*, 26. (d) Scheffer, A.; Engelhard, C.; Sperling, M.; Buscher, W. *Anal. Bioanal. Chem.* **2008**, *390*, 249. (e) Wahl, B.; Kloo, L.; Ruck, M. *Angew. Chem., Int. Ed.* **2008**, *47*, 3932. (f) Chaki, N. K.; Negishi, Y.; Tsunoyama, H.; Shichibu, Y.; Tsukuda, T. *J. Am. Chem. Soc.* **2008**, *130* (27), 8608. (f) Jiang, D.-e.; Tiago, M. L.; Luo, W.; Dai, S. *J. Am. Chem. Soc.* **2008**, *130*, 2777. (i) Mednikov, E. G.; Dahl, L. F. *Small* **2008**, *4*, 534.

(5) (a) Huang, C.-C.; Yang, Z.; Lee, K.-H.; Chang, H.-T. *Angew. Chem., Int. Ed.* **2007**, *46*, 6824. (b) Chen, S.; Ingram, R. S.; Hostetler, M. J.; Pietron, J. J.; Murray, R. W.; Schaaff, T. G.; Khoury, J. T.; Alvarez, M. M.; Whetten, R. L. *Science* **1998**, *280*, 2098. (c) Zheng, J.; Dickson, R. M. *J. Am. Chem. Soc.* **2002**, *124*, 13982. (d) Boyen, H.-G.; Kästle, G.; Weigl, F.; Ziemann, P.; Schmid, F.; Garnier, M. G.; Oelhafen, P. *Phys. Rev. Lett.* **2001**, *87*, 276401. (e) Huang, C.-C.; Chiang, C.-K.; Lin, Z.-H.; Lee, K.-H.; Chang, H.-T. *Anal. Chem.* **2008**, *80*, 1497. (f) Huang, C.-C.; Liao, H.-Y.; Shiang, Y.-C.; Lin, Z.-H.; Yang, Z.; Chang, H.-T. *J. Mater. Chem.* **2009**, *19*, 755. (g) Shiang, Y.-C.; Huang, C.-C.; Chang, H.-T. *Chem. Commun.* **2009**, 3437.

(6) (a) Bigioni, T. P.; Whetten, R. L.; Dag, ö. *J. Phys. Chem. B* **2000**, *104*, 6983. (b) Link, S.; Beeby, A.; FitzGerald, S.; El-Sayed, M. A.; Schaaff, T. G.; Whetten, R. L. *J. Phys. Chem. B* **2002**, *106*, 3410.

(7) (a) Lee, D. L.; Donkers, R. L.; Wang, G.; Harper, A. S.; Murray, R. W. *J. Am. Chem. Soc.* **2004**, *126*, 6193. (b) Negishi, Y.; Takasugi, Y.; Sato, S.; Yao, H.; Kimura, K.; Tsukuda, T. *J. Am. Chem. Soc.* **2004**, *126*, 6518. (c) Wang, G.; Huang, T.; Murray, R. W.; Menard, L.; Nuzzo, R. G. *J. Am. Chem. Soc.* **2005**, *127*, 812. (d) Zheng, J.; Zhang, C.; Dickson, R. M. *Phys. Rev. Lett.* **2004**, *93*, 077402. (e) Lin, C.-A. J.; Yang, T.-Y.; Lee, C.-H.; Huang, S. H.; Sperling, R. A.; Zanella, M.; Li, J. K.; Shen, J.-L.; Wang, H.-H.; Yeh, H.-I.; Parak, W. J.; Chang, W. H. *ACS Nano* **2009**, *3*, 395. (f) Zhou, R.; Shi, M.; Chen, X.; Wang, M.; Chen, H. *Chem.—Eur. J.* **2009**, *15*, 4944.

(8) (a) Kawata, S.; Kawata, Y. *Chem. Rev.* **2000**, *100*, 1777. (b) Polyzos, I.; Tsigaridas, G.; Fakis, M.; Giannetas, V.; Persephonis, P.; Mikroyannidis, J. *Chem. Phys. Lett.* **2003**, *369*, 264. (c) Parthenopoulos, D. A.; Rentzepis, P. M. *Science* **1989**, *245*, 843. (d) Belfield, K. D.; Schafer, K. J. *Chem. Mater.* **2002**, *14*, 3656.

(9) (a) He, G. S.; Bhawalkar, J. D.; Zhao, C. F.; Prasad, P. N. *Appl. Phys. Lett.* **1995**, *67*, 2433. (b) Ehrlich, J. E.; Wu, X. L.; Lee, I.-Y. S.; Hu, Z.-Y.; Röckel, H.; Marder, S. R.; Perry, J. W. *Opt. Lett.* **1997**, *22*, 1843. (c) Spangler, C. W. *J. Mater. Chem.* **1999**, *9*, 2013.

(10) (a) Kawata, S.; Sun, H.-B.; Tanaka, T.; Takada, K. *Nature* **2001**, *412*, 697. (b) Zhou, W.; Kuebler, S. M.; Braun, K. L.; Yu, T.; Cammack, J. K.; Ober, C. K.; Perry, J. W.; Marder, S. R. *Science* **2002**, *296*, 1106. (c) Cumpston, B. H.; Ananthavel, S. P.; Barlow, S.; Dyer, D. L.; Ehrlich, J. E.; Erskine, L. L.; Heikal, A. A.; Kuebler, S. M.; Lee, I.-Y. S.; McCord-Maughon, D.; Qin, J.; Röckel, H.; Rumi, M.; Wu, X.-L.; Marder, S. R.; Perry, J. W. *Nature* **1999**, *398*, 51.

(11) (a) Bhawalkar, J. D.; Kumar, N. D.; Zhao, C. F.; Prasad, P. N. *J. Clin. Laser Med. Surg.* **1997**, *15*, 201. (b) Ogawa, K.; Hasegawa, H.; Inaba, Y.; Kobuke, Y.; Inouye, H.; Kanemitsu, Y.; Kohno, E.; Hirano, T.; Ogura, S.-i.; Okura, I. *J. Med. Chem.* **2006**, *49*, 2276. (c) Kim, S.; Ohulchanskyy, T. Y.; Pudavar, H. E.; Pandey, R. K.; Prasad, P. N. *J. Am. Chem. Soc.* **2007**, *129*, 2669.

(12) (a) Kim, H. M.; Jung, C.; Kim, B. R.; Jung, S.-Y.; Hong, J. H.; Ko, Y.-G.; Lee, K. J.; Cho, B. R. *Angew. Chem., Int. Ed.* **2007**, *46*, 3460. (b) Wu, C.; Szymanski, C.; Cain, Z.; McNeill, J. *J. Am. Chem. Soc.* **2007**, *129*, 12904.

(13) (a) Tong, L.; Zhao, Y.; Huff, T. B.; Hansen, M. N.; Wei, A.; Cheng, J.-X. *Adv. Mater.* **2007**, *19*, 3136. (b) Imura, K.; Nagahara, T.; Okamoto, H. *J. Am. Chem. Soc.* **2004**, *126*, 12730. (c) Yelin, D.; Oron, D.; Thiberge, S.; Moses, E.; Silberberg, Y. *Opt. Express* **2003**, *11*, 1385. (d) Wang, H.; Huff, T. B.; Zweifel, D. A.; He, W.; Low, P. S.; Wei, A.; Cheng, J.-X. *Proc. Natl. Acad. Sci.* **2005**, *102*, 15752. (e) Imura, K.; Nagahara, T.; Okamoto, H. *Appl. Phys. Lett.* **2006**, *88*, 023104. (f) Imura, K.; Nagahara, T.; Okamoto, H. *J. Phys. Chem. B* **2005**, *109*, 13214. (g) Huff, T. B.; Tong, L.; Zhao, Y.; Hansen, M. N.; Cheng, J.-X.; Wei, A. *Nanomedicine* **2007**, *2*, 125. (h) Mühlschlegel, P.; Eisler, H.-J.; Martin, O. J. F.; Hecht, B.; Pohl,

D. W. *Science* **2005**, *308*, 1607. (i) Farrer, R. A.; Butterfield, F. L.; Chen, V. W.; Fourkas, J. T. *Nano Lett.* **2005**, *5*, 1139.

(14) (a) Ramakrishna, G.; Varnavski, O.; Kim, J.; Lee, D.; Goodson, T. *J. Am. Chem. Soc.* **2008**, *130*, 5032. (b) Patel, S. A.; Richards, C. I.; Hsiang, J.-C.; Dickson, R. M. *J. Am. Chem. Soc.* **2008**, *130*, 11602.

(15) (a) Imura, K.; Okamoto, H.; Hossain, M. K.; Kitajima, M. *Chem. Lett.* **2006**, *35*, 78. (b) Ueno, K.; Juodkazis, S.; Mizeikis, V.; Sasaki, K.; Misawa, H. *Adv. Mater.* **2008**, *20*, 26. (c) Durr, N. J.; Larson, T.; Smith, D. K.; Korgel, B. A.; Sokolov, K.; Ben-Yakar, A. *Nano Lett.* **2007**, *7*, 941.

(16) Liu, X.; Atwater, M.; Wang, J.; Huo, Q. *Colloids Surf., B* **2007**, *58*, 3.

(17) (a) Velusamy, M.; Shen, J.-Y.; Lin, J. T.; Lin, Y.-C.; Hsieh, C.-C.; Lai, C.-H.; Lai, C.-W.; Ho, M.-L.; Chen, Y.-C.; Chou, P.-T.; Hsiao, J.-K. *Adv. Funct. Mater.* **2009**, *19*, 1. (b) Zhang, P.; Sham, T. K. *Appl. Phys. Lett.* **2002**, *81*, 736. (c) Brandys, M.; Jennings, M. C.; Puddephatt, R. J. *J. Chem. Soc., Dalton Trans.* **2000**, 4601.

(18) Chou, C.-F.; Huang, T.-H.; Lin, J.-T.; Hsieh, C.-C.; Lai, C.-H.; Chou, P.-T.; Tsai, C. *Tetrahedron* **2006**, *62*, 8467.

(19) (a) Albota, M. A.; Xu, C.; Webb, W. W. *Appl. Opt.* **1998**, *37*, 7352. (b) Xu, C.; Webb, W. W. *J. Opt. Soc. Am. B* **1996**, *13*, 481.

(20) Fisher, W. G.; Wachter, E. A.; Lytle, F. E.; Armas, M.; Seaton, C. *Appl. Spectrosc.* **1998**, *52*, 536.

(21) (a) Sheik-Bahae, M.; Said, A. A.; Wei, T.-H.; Hagan, D. J.; Van Stryland, E. W. *IEEE J. Quantum Electron.* **1990**, *26*, 760. (b) Swiatkiewicz, J.; Prasad, P. N.; Reinhardt, B. A. *Opt. Commun.* **1998**, *157*, 135. (c) Lee, S.; Pérez-Luna, V. H. *Anal. Chem.* **2005**, *77*, 7204. (d) Pawlicki, M.; Collins, H. A.; Denning, R. G.; Anderson, H. L. *Angew. Chem., Int. Ed.* **2009**, *48*, 3244.

(22) (a) Menard, L. D.; Xu, H.; Gao, S.-P.; Twesten, R. D.; Harper, A. S.; Song, Y.; Wang, G.; Douglas, A. D.; Yang, J. C.; Frenkel, A. I.; Murray, R. W.; Nuzzo, R. G. *J. Phys. Chem. B* **2006**, *110*, 14564. (b) Guo, R.; Murray, R. W. *J. Am. Chem. Soc.* **2005**, *127*, 12140.

(23) (a) Negishi, Y.; Tsukuda, T. *Chem. Phys. Lett.* **2004**, *383*, 161. (b) Huang, T.; Murray, R. W. *J. Phys. Chem. B* **2001**, *105*, 12498. (c) Negishi, Y.; Nobusada, K.; Tsukuda, T. *J. Am. Chem. Soc.* **2005**, *127*, 5261. (d) Zheng, J.; Petty, J. T.; Dickson, R. M. *J. Am. Chem. Soc.* **2003**, *125*, 7780. (e) Tran, M. L.; Zvyagin, A. V.; Plakhotnik, T. *Chem. Commun.* **2006**, 2400. (f) Shi, X.; Ganser, T. R.; Sun, K.; Balogh, L. P.; Baker, Jr, J. R. *Nanotechnology* **2006**, *17*, 1072. (g) Duan, H.; Nie, S. *J. Am. Chem. Soc.* **2007**, *129*, 2412. (h) Yang, Y.; Chen, S. *Nano Lett.* **2003**, *3*, 75. (i) Ramakrishna, G.; Dai, Q.; Zou, J.; Huo, Q.; Goodson III, T. *J. Am. Chem. Soc.* **2007**, *129*, 1848.

(24) Huang, T.; Murray, R. W. *J. Phys. Chem. B* **2003**, *107*, 7434.

(25) Pu, S.-C.; Yang, M.-J.; Hsu, C.-C.; Lai, C.-W.; Hsieh, C.-C.; Lin, S. H.; Cheng, Y.-M.; Chou, P.-T. *Small* **2006**, *2*, 1308.

(26) Bautista, M. C.; Bomati-Miguel, O.; Morales, M. P.; Serna, C. J.; Veintemillas-Verdaguer, S. *J. Magn. Magn. Mater.* **2005**, *293*, 20.

(27) Uchugonova, A.; König, K. *J. Biomed. Opt.* **2008**, *13*, 054068.

(28) Panyam, J.; Zhou, W. Z.; Prabha, S.; Sahoo, S. K.; Labhasetwar, V. *FASEB J.* **2002**, *16*, 1217.

JP9080492